Polar Biol (2010) 33:1641–1650
DOI 10.1007/s00300-010-0839-3

ORIGINAL PAPER

Primary production and climatic variability in the European sector of the Arctic Ocean prior to 2007: preliminary results

Paul Wassmann · Dag Slagstad · Ingrid Ellingsen

Received: 29 October 2009 / Revised: 29 April 2010 / Accepted: 23 May 2010 / Published online: 22 June 2010

Abstract The primary production in the Greenland Sea, Fram Strait, Barents Sea, Kara Sea and adjacent Polar Ocean was investigated through the physically–biologically coupled, nested 3D SINMOD model with 4 km grid size for the years 1995–2007. The model had atmospheric forcing from the European Centre for Medium-Range Weather Forecasts (ECMWF) reanalysis data. Three basic gross primary production (GPP) domains were distinguished: (i) an extensive domain dominated by Atlantic Water, (ii) an elongated domain roughly corresponding to the seasonal ice zone (SIZ) and (iii) a compact perennial ice zone (>100, between 100 and 30 and <30 g C m^{-2} $year^{-1}$, respectively). The interannual coefficient of variation for GPP in domain (i) was <0.1, and increased northwards towards >0.6 in the northwesternmost and northeasternmost fringe of the SIZ. The primary production in the northern sector of the European Arctic Corridor (EAC) region prior to 2007 was characterised by limited interannual variability, on average 75.2 ± 10% and 24.0 ± 16% g C m^{-2} $year^{-1}$ for the EAC region at 74–80 and >80°N, respectively. The main primary production anomalies were found early in the productive season and in sections of the SIZ, generally in regions with low GPP. There was no significant trend of increasing GPP in the 1995–2007 time interval.

P. Wassmann (✉)
Institute of Arctic and Marine Biology,
University of Tromsø, 9037 Tromsø, Norway
e-mail: paul.wassmann@uit.no

D. Slagstad · I. Ellingsen
SINTEF Fisheries and Aquaculture,
7465 Trondheim, Norway

Keywords European Arctic Ocean · Primary production · Seasonal ice zone · Global warming · Interannual decadal variability · Decadal anomalies

Introduction

The Polar Regions are predicted to incur some of the most pronounced effects of global climate change (ACIA and Loeng 2005). The spectacular acceleration of Arctic ice loss in 2007, and the ensuing recovery in 2008 and 2009 towards the overall negative 1979–2006 trend line, suggests that the Arctic Ocean may experience rapid environmental changes (Stroeve et al. 2007; Comiso et al. 2008). Moreover, the Arctic is warming about 2–3 times faster than the global rate (ACIA and Loeng 2005; Trenberth et al. 2007), and changes are likely to be seen much earlier there than in other regions. Thus, Arctic ecosystems may encounter climate-driven thresholds or tipping points in the near future. Indeed, the Arctic ice pack has been identified as one of the key tipping elements in the world climate system, making change in the Arctic significant on a global scale.

The European sector of the Arctic Ocean, i.e. the European Arctic Corridor (EAC), stretching from the Fram Strait in the west to the northern Kara Sea in the east, is of utmost significance for the oceanography and ecology of the Arctic Ocean (Fig. 1). Far more than 50% of the total primary production of the Arctic Ocean takes place here (Sakshaug 2004; Pabi et al. 2008). The inflow of Pacific Water to the Arctic Ocean contributes only about 10–13% of total inflow. Of inflowing Atlantic Water, 1.1 Sv (S > 35 pps) enters the Barents Sea (Skagseth 2008) and leaves subducted below Arctic Water through the St. Anna Trough, while 5–8 Sv flows northwards along the continental shelf of West-Spitsbergen into the Arctic Ocean

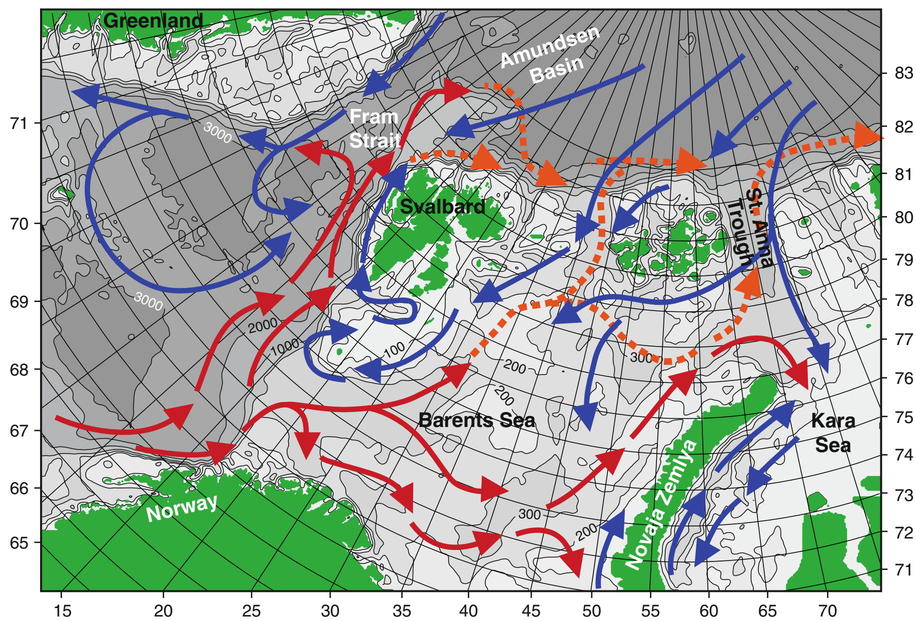

Fig. 1 The European Arctic Corridor region consisting of the Fram Strait, Barents Sea, Kara Sea and the adjacent Arctic Ocean. Latitudes from 61 to 83°N and longitudes from 15 to 70°E are indicated. Also shown are the main Atlantic (*red*) and Arctic (*blue*) currents. *Stippled* and *reddish lines* indicate subduction of Atlantic Water below the Arctic surface water

(Schauer et al. 2004; Holfort and Hansen 2005). An indeterminate fraction of this Atlantic Water is recycled in the Fram Strait, but approximately 5 Sv enters the Arctic Ocean subducted north of Spitsbergen. More than 80% of the outflow of Arctic Water from the Arctic Ocean basins leaves through western Fram Strait. The EAC region thus plays a pivotal role for the Arctic Ocean climatology as 80% or more of both the in- and outflow takes place here (Fig. 1).

For the waters around Svalbard (e.g. Hop et al. 2006) and the central Barents Sea (e.g. Wassmann et al. 2006b), sufficient oceanographic process knowledge and data have accumulated to validate models (e.g. Slagstad and McClimans 2005; Wassmann et al. 2006a; Ellingsen et al. 2009). For the remaining seas, however, data are scarce (Kara Sea, but see Hirche et al. 2006; Fram Strait, but see Hop et al. 2006) or essentially non-existent (Nansen and Amundsen Basin). Some poorly studied areas are difficult to access (eastern Barents Sea, but see Kuznetsov and Schoschina 2003); others are the subject of ongoing investigations (e.g. Fram Strait, iAOOS project [www.iaoos.no]). Ecological models for the EAC region can thus not be validated with extensive, balanced data sets, except for remotely sensed ice cover. Concurrently, important questions are being asked, for example how climate change affects the C flux and ecosystem development in the Arctic Ocean. These questions are usually addressed through global climate models with limited ability to provide adequate coverage on a regional scale.

As a first step towards finding answers regarding the C cycling in a defined region of the Arctic Ocean, the algorithms of the regional SINMOD model, developed and validated for the Barents Sea (for details see Slagstad and McClimans 2005; Wassmann et al. 2006a), were extrapolated to the entire EAC domain. These results must thus be considered preliminary until good quality and sufficient validation measurements are available. Considering the vastness of the EAC region, and the logistic challenges posed by its ice cover, we are unlikely to acquire sufficient in situ measurements in the near future. However, as the EAC region is crucial for an understanding of the present and future climatic development in the Arctic Ocean, one may have no other choice than to work with inadequately validated models in order to shed light on prominent questions, such as spatial features, magnitude and time variation of fundamental biological processes. As an alternative, one could perform rigorous sensitivity analysis of the most critical factors for gross primary production (GPP), e.g. ice cover and thickness, vertical stability and mixing for the start of the spring bloom, intensity and composition of atmospheric light (e.g. frequent fog events), biological parameters of phytoplankton groups, etc. This is a complex task, demanding extensive research funds and computer time. Nevertheless, approximating where, when and how changes in C flux take place is a matter of urgency.

In order to assess the effects of a declining summer ice cover in the Arctic Ocean and increasing temperature of the Atlantic water inflow through the EAC region, we present some first results regarding the GPP for the period 1995–2007, i.e. for the decade prior to the acceleration of Arctic ice loss in 2007. This investigation thus creates a base for comparison and to evaluate GPP developments in a future ice-free Arctic Ocean in late summer. How did annual GPP vary in the EAC region prior to 2007? Where and how extensive were the decadal GPP anomalies in the region? Is there a trend towards increased GPP prior to 2007?

Materials and methods

In a remote, vast and inaccessible region such as the EAC, the only practical method to address the question of primary production and C flux over the entire region is to apply mathematical models, developed on and validated by existing measurements on the physical, chemical and biological oceanography of the area. The results presented here derive from the CABANERA project (see Wassmann et al. 2008), and they rely upon SINMOD, a coupled hydrodynamic-ice-chemical-ecosystem model system. Here we expand on earlier model contributions that focussed upon the Barents Sea region (detailed description: Slagstad and McClimans 2005; Wassmann et al. 2006a) by extending the model domain to the Fram Strait, the northern Barents and Kara Seas and the Arctic Ocean shelf break (Fig. 2). The large-scale model has a horizontal grid point distance of 20 km and the nested model 4 km for the years 1995–2007 (see Fig. 2). Atmospheric forcing has been provided by the European Centre for Medium-Range Weather Forecasts (ECMWF) (ERA-40 from 1979 to 2002 and ECMWF_OPER beyond 2002). The model is also forced with freshwater fluxes (river discharges and diffuse run-off from land), based on data from a simulation with a hydrological model [see Dankers and Middelkoop (2008) for details]. Four tidal components (M_2, S_2, K_1 and N_2) are imposed by specifying the various components at the open boundaries of the large-scale model (from the tidal model TPXO 6.2, http://www.coas.oregonstate.edu/research/po/research/tide/index.html). Ice dynamics and the hydrodynamic performance are described in Ellingsen et al. (2009). The model reproduces ice cover and hydrodynamic conditions fairly well, and its performance is improved compared to the previous version described by Slagstad and McClimans (2005). The ecosystem module includes nitrate, ammonium, silicate, diatoms, flagellates, microzooplankton, bacteria, heterotrophic nanoflagellates, fast sinking detritus, slow sinking detritus (Slagstad et al. 1999) and the two dominant key zooplankton species *Calanus finmarchicus* (Atlantic) and *C. glacialis* (Arctic) (Slagstad and Tande 2007). This part of the model was presented in detail by Wassmann et al. (2006a), and some features of the biological model are also evaluated in Ellingsen et al. (2008).

Results

Average decadal, annual gross primary production

The average annual estimates of GPP for the period 1995–2007 range from rates around 20 to >160 g C m^{-2} (Fig. 3). Under the influence of Atlantic Water supply, GPP is highest along the eastern Norwegian Coast, the Norwegian Sea, the eastern Fram Strait and the central and southern Barents Sea. GPP is of course lowest in the central Arctic Ocean and in the northern and central Kara Sea due to continuous ice cover. In these latter regions, ice algae will add to GPP, but the model does not quantify their contribution. Between these two regions we find the expanse of the seasonal ice zone (SIZ), which is particularly wide in the western Fram Strait and the northern Barents Sea. Here, GPP ranges between 50 and 100 g C m^{-2}.

The spatial distribution of the annual GPP in the EAC region appears uncomplicated and characterised by smooth,

Fig. 2 The model domain. In the *upper right* the main model domain and the nested area of the European Arctic Corridor for which gross primary production results are presented. Also shown are the regions above 74 and 80°N for which separate estimates of gross primary production are provided

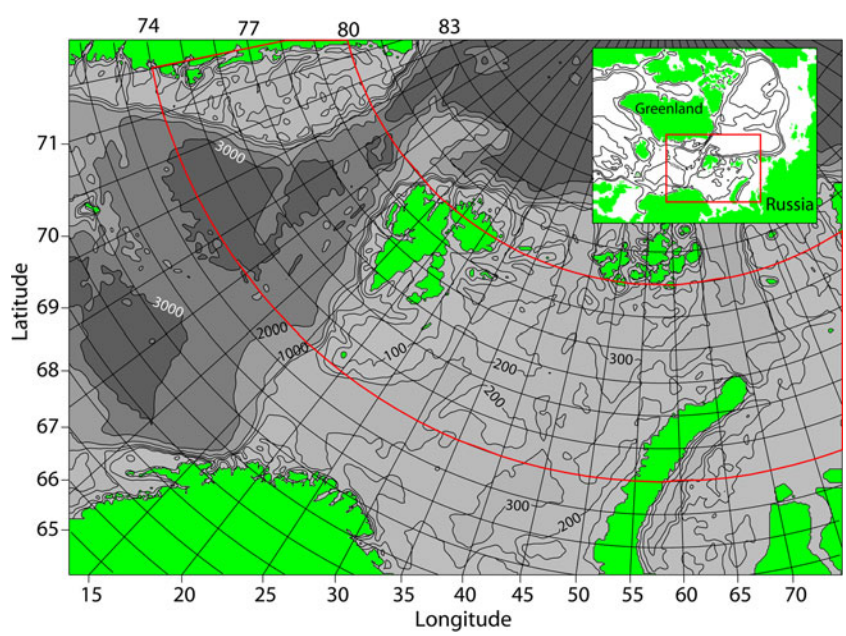

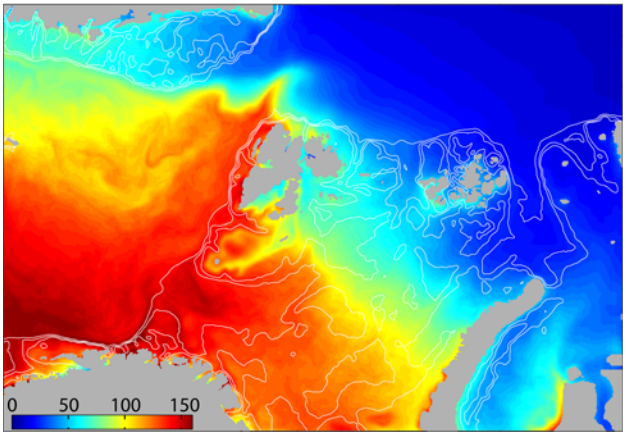

Fig. 3 The average gross primary production in the European Arctic Corridor for the period 1995–2007. *Scale* to the *left* (g C m^{-2} $year^{-1}$)

straightforward isolines. The reason for this is that Fig. 3 represents the average of 13 years. While the basic patterns are similar from year to year, there is substantial spatial difference between the various years (Fig. 4). As expected, years with less ice cover show higher GPP rates than years with more extensive ice cover, but the model also simulates considerable small scale spatial variability with eddies and fronts (Fig. 4).

Decadal gross primary production anomalies

The coefficient of variation (standard deviation/mean) of annual GPP in the EAC for the 1995–2007 time interval is presented in Fig. 5. It ranges from low ratios well below 0.1 up to maximum ratios of about 0.6 (see also Fig. 9). For the regions dominated by Atlantic Water with the highest GPP, the coefficient of variation is the lowest, <0.1. In the adjacent ice-covered regions, the conditions are more complex. Most of the SIZ in the Fram Strait and the Barents Sea is characterised by coefficients of variation around 0.2. Similar coefficients are also encountered in much of the Nansen Basin north of Svalbard. Annual coefficients of variation of >0.3 are found off northwestern Greenland, north of Spitsbergen, the northeastern Barents Sea, around Franz Josef Land and in the northern Kara Sea. The highest coefficients of variation are frequently found in relatively shallow regions and the southeastern Kara Sea with low annual GPP

Fig. 4 The gross primary production in the European Arctic Corridor for the years 2007 (**a**), 2005 (**b**), 2003 (**c**), 2001 (**d**), 1999 (**e**) and 1997 (**f**). *Scale* to the *left* (g C m^{-2} $year^{-1}$)

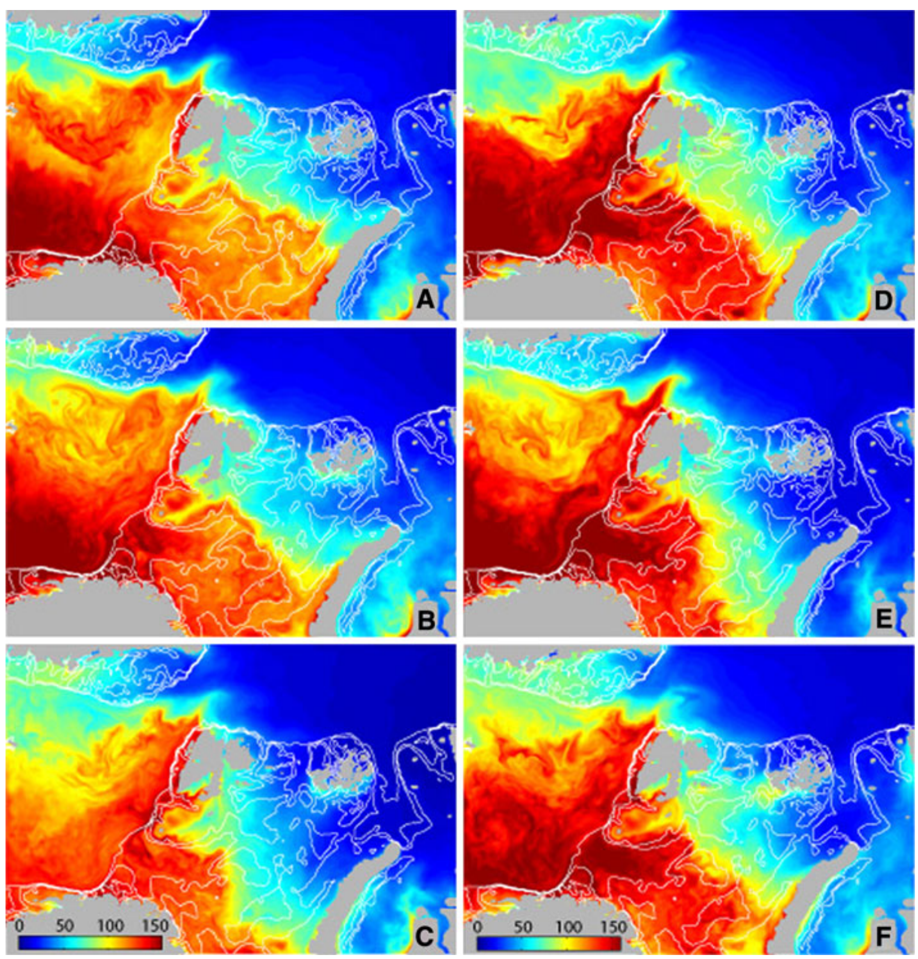

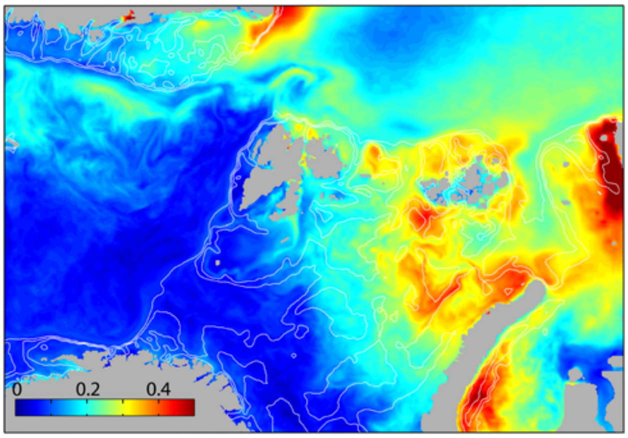

Fig. 5 The coefficient of variation (standard deviation/mean) of the annual gross primary production in the European Arctic Corridor for the period 1995–2007. *Scale* to the *right*. Please note that the annual is smaller than the monthly decadal coefficient of variation (Figs. 6, 7)

(compare Figs. 3, 5). Ice algae GPP (not quantified by the model) will add to total GPP and may have had an influence on GPP anomalies.

Average decadal, monthly gross primary production and anomalies

The rapid increase in GPP from April to May and its culmination in June are illustrated in Fig. 6 (left column, a–c). In the Arctic domain influenced by Atlantic water north of 77°N, GPP increases from at most 8 to >40 g C m^{-2} $month^{-1}$. At the start of the productive period, GPP is small in the Arctic. In May GPP accelerates in the southern Barents Sea, the northern Norwegian Sea and along the west-Spitsbergen shelf. June is noticeably the GPP climax, with high rates over most of the EAC region dominated or influenced by Atlantic water, including the southern sectors of the SIZs of the Fram Strait and Barents Sea.

The monthly coefficients of variation suggest some noteworthy patterns. Monthly variability is clearly far greater than annual variability (compare the scales of Figs. 4, 5, 6). The variability at the beginning of the productive period, i.e. April and May, is very high, being highest along the SIZs of the Fram Strait and the Barents Sea, north of Spitsbergen and north of Franz Josef Land (Fig. 6d–f, right

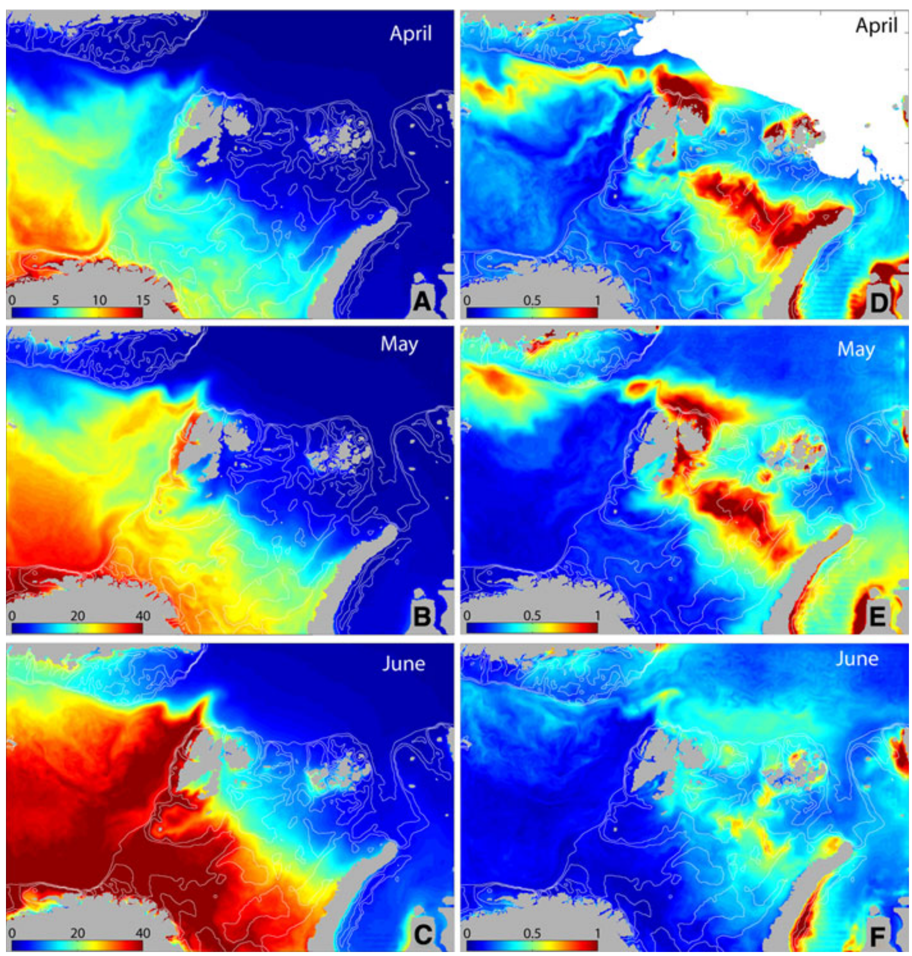

Fig. 6 *Left column*: Monthly average gross primary production in the European Arctic Corridor for the period 1995–2007 and the months April (**a**), May (**b**) and June (**c**). *Scale* to the *left* (g m^{-2} $month^{-1}$). *Right column*: Coefficient of variation of the monthly decadal gross primary production in the European Arctic Corridor for the period 1995–2007 and the months April (**d**), May (**e**) and June (**f**). *Scale* to the *left*. Observe the difference in scales between Figs. 5 and 6. The coefficients of variation in the Nansen Basin for April **d** have been left out because extremely low primary production rates support unreasonable coefficients of variability

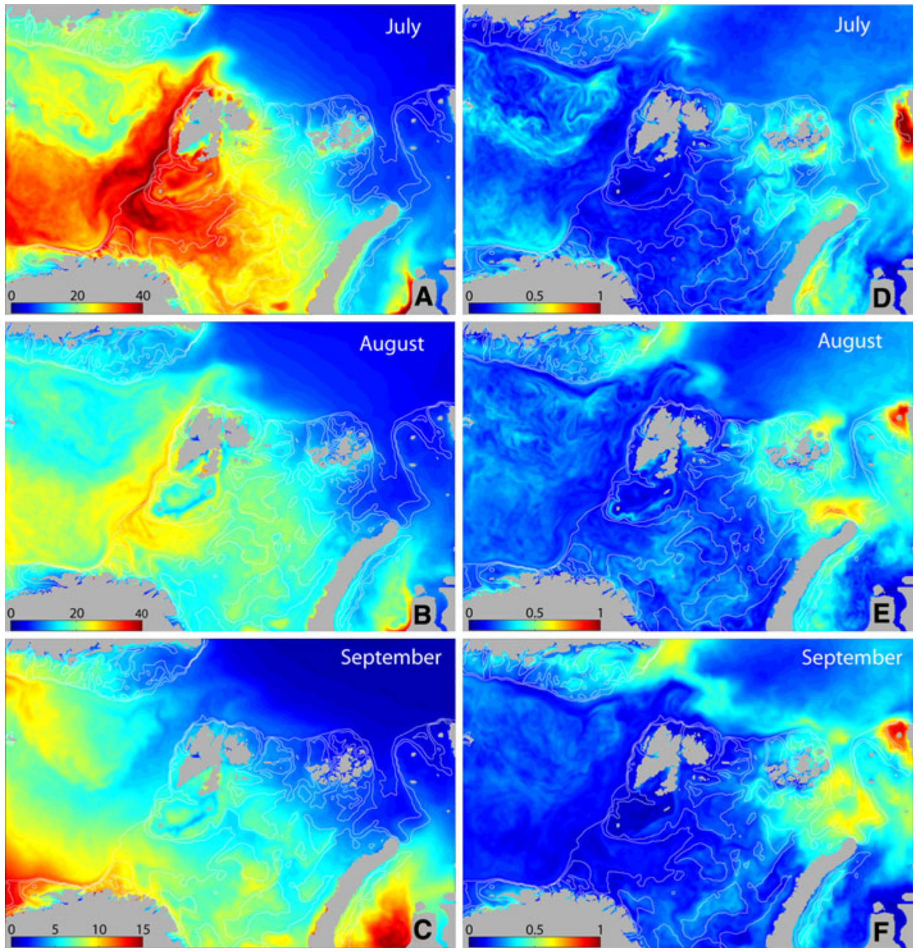

Fig. 7 *Left column*: Monthly average gross primary production in the European Arctic Corridor for the period 1995–2007 and the months July (**a**), August (**b**) and September (**c**). *Scale* to the *right* (g m^{-2} $month^{-1}$). *Right column*: Coefficient of variation of the monthly decadal gross primary production in the European Arctic Corridor for the period 1995–2007 and the months July (**d**), August (**e**) and September (**f**). *Scale* to the *right* (standard deviation/mean). Observe the difference in scales between Figs. 5 and 6

column). In June, the coefficient of variation decreases drastically throughout the model domain, with coefficients around 0.5 in the central and north of the Barents Sea and maxima in the southeastern and northeastern Kara Sea.

In July, the GPP is already clearly reduced, when compared with June (Fig. 7a–c, left column; 30–40 g C m^{-2} $month^{-1}$). The effect of the Atlantic Water flowing along the shelf break northwards and into the Barents Sea is clearly visible. GPP increases even into the Arctic Ocean and north of Svalbard. By August, most of the GPP has declined to rather low levels, but evenly distributed rates through the region (often around 20 g C m^{-2} $month^{-1}$). Again, the Atlantic inflow can be discerned, as well as the low GPP on the Svalbard Bank and Spitsbergen inshore waters, which reflects stratification and nutrient depletion. Also, the influence of the Jan Mayen current, transporting modified Arctic water across the Fram Strait towards the northward-flowing Atlantic water off Spitsbergen is clearly reflected in GPP in July to September. By September, the productive season is coming to an end. Characteristic for July to September is that the GPP coefficients of variation are well below 0.5 for most of the EAC region, with coefficients >0.5 in the low-productive regions northeast of Greenland, the northeastern Barents Sea and the northern Kara Sea (Fig. 7d–f, right column).

Temporal variability in the annual gross primary production

The annual GPP in the entire EAC model domain varies from year to year, ranging between about 66 and 89, with an average GPP of 76.5 ± 5.6 C g m^{-2} $year^{-1}$ (Fig. 8). In the more Arctic section between 74 and 80°N (Fig. 2), the average GPP is not very different from that of the entire EAC model domain: 75.2 ± 7.2 g C m^{-2} $year^{-1}$ (Fig. 8). The mean annual GPP in the High Arctic EAC domain >80°N (Fig. 2) was on average 24.0 ± 3.5 g C m^{-2} $year^{-1}$ (Fig. 8).

Ice cover is the main cause of the variability and periods of increased (2006) and decreased (2003) GPP. However, in none of the three sectors of the model domain show any particular trend in temporal variability of annual GPP estimates, not even the High Arctic domain north of 80°N. This suggests that neither the slow but steady decrease of ice cover observed in the entire Arctic Ocean in the years 1995–2007 nor the rapid decline in 2007 had any effect on GPP in the EAC region.

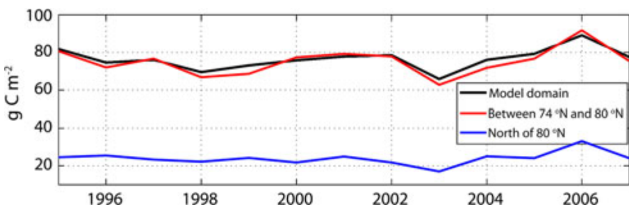

Fig. 8 Variability in annual phytoplankton gross primary production (g C m^{-2}) between 1995 and 2007 for the European Arctic Corridor. The rates for the entire model domain (*black*), the region 74–80°N (*red*) and >80°N (*blue*) are denoted

Discussion

Although ice cover and ice transport have declined in recent decades in regions such as the Fram Strait and the Barents Sea (Vinje 2001; Rodrigues 2008), the changes are clearly smaller than in other Arctic regions. While ice cover has decreased significantly in the entire Arctic Ocean since 2006 (in particular in the Beaufort, Chukchi and East Siberian Seas, see Stroeve et al. 2007), there has simultaneously been more ice than normal north of Spitsbergen and in the Fram Strait. During 2007 when the Arctic Ocean ice cover shrank to record lows, there was more ice than usual average north of Spitsbergen and the Fram Strait (see Arrigo et al. 2008). More ice cover in a time of significant ice reduction is no contradiction, but part of an inherent spatial and regional variability of the Arctic Ocean. It is thus not surprising that there is no significant trend in the annual GPP variation over time in the EAC region (Fig. 8). It is worthwhile noting that the only region where Arrigo et al. (2008) recorded a decline in GPP in 2007 (when compared to the 1998–2002 average) was in the Greenland Sea and the adjacent northern Barents Sea region. The ice cover in the EAC region is currently increasing slightly, rather than decreasing.

Ice algae are found in highly variable concentrations throughout the EAC region (e.g. Ratkova and Wassmann 2005), and there are few space-integrated estimates for ice algae GPP (e.g. McMinn and Hegseth 2006). For the entire Barents Sea, the maximum contribution by ice algae to GPP (5.3 g C m^{-2}; Hegseth 1998) has been calculated to represent 4% of the GPP (Wassmann et al. 2006b). However, in the most heavily ice-covered northern regions, the relative contribution from ice algae is higher (e.g. Gosselin et al. 1997). Total GPP in the model could therefore be underestimated because the GPP of ice algae is missing. This has ramification for the interpretation of the ecological consequences deriving from GPP anomalies. However, particularly during conditions of heavy ice cover, GPP is critically dependent on photosynthetic active radiation (PAR). Ice algae scavenge PAR that penetrates the ice and snow cover and thus reduce the GPP sustained by phytoplankton. In the absence of ice algae in the model, PAR penetrating the ice is fully available for phytoplankton, which to an unknown degree compensates for the lack of ice algae primary production in the model.

The hydrodynamics and primary production regime of a region is influenced by whether or not the sea is ice-covered. During the productive season, the EAC is characterised by a lack of major polynyas. The North East Water Polynya has more or less disappeared. The Storfjord Polynya is usually open in winter. Short-lived polynyas open up depending on wind strength and direction. This lack and the minimal contribution of freshwater by rivers in the EAC region means that GPP can basically be divided into three large domains: (i) a vertically mixed, southern domain and West-Spitsbergen that develops a weak thermal stratification in late summer, (ii) a strongly stratified northern domain (SIZ) that is decreasingly exposed to PAR and (iii) a perennially ice-covered region north of about 80°N. These three domains are roughly delineated by the 100 and 30 g C m^{-2} $year^{-1}$ isolines (Fig. 3). The regions (i), (ii) and (iii) exhibit GPP rates of approximately >100, 100 to 30 and <30 g C m^{-2} $year^{-1}$, respectively.

The Svalbard Bank region belongs geographically to the ice-covered domain (ii) but belongs functionally to (i). Strong tidal mixing and shelf-edge upwelling, both of which are topographically induced are the cause of the high GPP of Svalbard Bank (Fig. 7). The GPP in the EAC region is mainly a question of PAR (ice cover) and nutrient supply (winter accumulated concentrations and vertical mixing) while additional upwelling events and advection of nutrients result in more complex PAR/nutrient/GPP relations in some regions of the Arctic Ocean (Tremblay and Gagnon 2009). While the ongoing rise in the supply of heat and freshwater in and to the Arctic Ocean should strengthen vertical stratification in ice-covered regions, episodic atmospheric events (e.g. low pressure passage) may act in synergy with prolonged exposure to light and increased pelagic productivity, thus increasing the GPP overall. Atmospheric forcing is a significant determinant of GPP in the non-stratified regions of EAC (e.g. Sakshaug 2004; Wassmann et al. 2004) but will in the future be more prominent along the entire southern, circumpolar rim of the pan-Arctic SIZ. Here, stratification is less strong and atmospheric forcing can result in erosion of vertical stability. Thus, the GPP realm (i) will slowly expand northwards as winter ice cover spreads less southwards due to the storm-induced erosion of vertical stability.

Ice cover is by far the single most important factor for GPP in the Arctic Ocean. Recently, Ellingsen et al. (2009) demonstrated that the correlation between annual and modelled ice cover in the Barents Sea and adjacent regions is good ($R^2 = 0.88$). With regard to the most prominent source

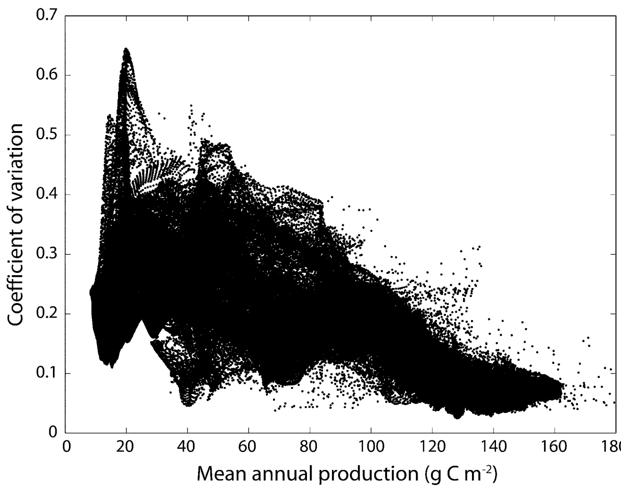

Fig. 9 Coefficient of variation as a function of annual phytoplankton gross primary production for the period 1995–2007 in the entire model domain. Note the high coefficients *and* the large variability at low annual rates of phytoplankton gross primary production

of GPP variability, i.e. the interannual variation in ice cover, there is therefore relatively good agreement between our model and nature. Ice cover also has ecological consequences for the ecosystem compartments that exist in the most ice-covered sectors of the SIZ. A shrinking and thinning future ice cover will result in the establishment of provinces with increased productivity.

Figure 9 illustrates the relationship between average annual GPP and the coefficient of variation for the period 1995–2007. The overall relationship is negative. But, more importantly, the variability among the coefficients of GPP variation is highest at low GPP and declines with increasing annual GPP rates. This suggests that GPP, the base for any further plankton ecosystem development, varies the most in the northernmost SIZ and more isolated regions where highly variable ice cover permits sufficient light penetration. This high variability in GPP in the borderland regions between partly open and permanently ice-covered waters implies that only organisms that can cope with such erratic living conditions can establish more lasting populations. The ice margins with their long-term or short-term variability are difficult regions for long-lived and newly arrived heterotrophic organisms to establish themselves in. Examining the lowest GGP rates in Fig. 9 in greater detail, one can note that the coefficients of variation reach a maximum around 20 g C m^{-2} $year^{-1}$, but that variability drops sharply towards 10 g C m^{-2} $year^{-1}$. This suggests that the regions with the lowest rates of GPP in the Arctic Ocean are presently subject to a small variability but that this may increase sharply in the near future. However, the model also reaches precision limits at low GPP rates and the computational errors may be large.

Current ice models suggest that the Arctic Ocean will be largely ice-free in late summer in 2 decades, with a cover of mostly first-year ice in winter (Stroeve et al. 2007). In addition, the average thickness of sea ice has decreased steadily (Giles et al. 2008; Rothrock et al. 2008), whereas increases have been reported in the amount of freshwater stored in the Atlantic (McPhee et al. 2009), the transport of ice and freshwater towards the Fram Strait (von Eye et al. 2009) and the melting probability of sea ice. Such extensive changes in sea ice dynamics and the ongoing declines in perennial ice cover (Nghiem et al. 2007) will necessarily have effects on Arctic ecosystems, both with regard to climatic feedbacks, ecosystem structure and function, and of course GPP. Arrigo et al. (2008) estimated that the GPP of the Arctic Ocean increased by 23% from the 1998–2002 average to 2007, in particular in the Canadian Basin and off eastern Siberia. While major regions in the Arctic Ocean become ice-free in summer, the thinner annual ice drifts more quickly than in previous times. For example, the recent drift of RV Tara over the Arctic Ocean with the Transpolar Drift took only half as long as the same journey took RV Fram in 1894. Ice, thinner than previously, is thus more easily transported than before over the Arctic Ocean towards northern Greenland, the Fram Strait and northern Svalbard (von Eye et al. 2009).

While increased GPP has already been modelled/observed in many of the regions of the Arctic Ocean that have become ice-free in summer (e.g. Arrigo et al. 2008) increased ice drift towards Svalbard and the Fram Strait prohibits major increases in GPP in the EAC region. Major increases in GPP in the EAC region are thus not expected until the ice drift towards Svalbard and through the western Fram Strait declines. This will probably happen only when most of the Arctic has become ice-free. GPP will naturally increase proportionally with the wane of ice cover (e.g. Arrigo et al. 2008), but stratification due to freshwater storage (McPhee et al. 2009) will impose nutrient limitation and thus limit new production. The situation in the EAC region must thus be interpreted in light of the regional peculiarities of the Arctic Ocean where changes in GPP differ from those occurring in the Pacific sector.

The recent acceleration of Arctic ice loss, the thinning of the ice and the decline of the multiyear sea ice suggests that the Arctic Ocean may face rapid changes in basic ecosystem function. Future changes in ecosystem function and biogeochemical cycling have to be compared to some standard, e.g. the time prior to 2007. The model run for the years 1995–2007 creates a baseline for comparison of future climate scenarios in the EAC region. From this perspective and for comparative reasons, the current GPP estimates have their merits, despite being inadequately validated.

Global climate models are limited in their ability to provide reliable, regional-scale projection of various climate variables. With the SINMOD model, we try to improve the understanding of regional processes, the role of short-lived climate forcers and local climate impacts by examining the GPP during the past decade in the EAC region. Regional models are indispensible to improve the realism in global C flux and climate models. Improved regional-scale models and projections will help to bridge the gap between global studies and models and local impacts and changes in the Arctic Ocean.

In conclusion, the GPP in the EAC region prior to 2007 appears characterised by limited interannual variability, on average 75.2 ± 10% and 24.0 ± 16% g C m^{-2} $year^{-1}$ for the EAC region (74–80 and >80°N, respectively). The decadal GPP anomalies in most of the EAC region seem small, in particular in the regions dominated by Atlantic Water. The biggest monthly anomalies were found in those parts of the SIZ that lose ice early in the season, a region of high GPP. In contrast, the biggest annual anomalies were encountered in the SIZ that loses ice late in the season (low GPP). Due to the low GPP rates, the highest coefficients of GPP variation have to be interpreted with care as they could be more mathematical than ecological in nature. When speculating where, when and how the largest relative changes in GPP can be expected in EAC region in the near future, the GPP anomalies may be our guide. There is no significant trend of increased GPP in the time prior to 2007 and the present investigations can thus serve as a baseline for eventual future changes in GPP.

Acknowledgments This work was supported by the project *Carbon flux and ecosystem feedback in the northern Barents Sea in an era of climate change* (CABANERA, Research Council of Norway, Norklima programme, grant # 155936/700). Additional support came from the European Union through the project *Arctic Tipping Points* (ATP, contract # 226248, www.eu-atp.org) in the framework FP7 and from the Norwegian Research Council through its International Polar Year programme and the project *iAOOS-Norway—Closing the Loop* (grant # 176096/S30; http://www.iaoos.no).

References

ACIA, Loeng H (2005) Marine systems. In: Symon C, Arris L, Heal B (eds) Arctic climate impact assessment. Cambridge University Press, New York, pp 453–538

Arrigo KR, van Dijken G, Pabi S (2008) Impact of shrinking Arctic ice cover on marine primary production. Geophys Res Lett 35:L19603

Comiso JC, Parkinson CL, Gersten R, Stock L (2008) Accelerated decline in the Arctic sea ice cover. Geophys Res Lett 35:L01703

Dankers R, Middelkoop H (2008) River discharge and freshwater runoff to the Barents Sea under present and future climate conditions. Clim Change 87:131–153

Ellingsen IH, Dalpadado P, Slagstad D, Loeng H (2008) Impact of climatic change on the biological production in the Barents Sea. Clim Change 87:155–175

Ellingsen I, Slagstad D, Sundfjord A (2009) Modification of water masses in the Barents Sea and its coupling to ice dynamics: a model study. Ocean Dyn. doi:10.1007/s10236-009-0230-5

Giles KA, Laxon SW, Ridout AL (2008) Circumpolar thinning of Arctic sea ice following the 2007 record ice extent minimum. Geophys Res Lett 35:L22502

Gosselin M, Levasseur M, Wheeler PA, Horner RA, Booth BC (1997) New measurements of phytoplankton and ice algal production in the Arctic Ocean. Deep Sea Res 44:1623–1644

Hegseth EN (1998) Primary production of the northern Barents Sea. Polar Res 17:113–123

Hirche H-J, Kosobokova KN, Harms I, Meon B, Nöthig E-M (2006) The pelagic systems of the Kara Sea—communities and components of the carbon flow. Prog Oceanogr 7:291–316

Holfort J, Hansen E (2005) Time series of Polar Water properties in Fram Strait. Geophys Res Lett 32:L19601

Hop H, Falk-Petersen S, Svendsen H, Kwasniewski S, Pavlov V, Pavlova O, Søreide JE (2006) Physical and biological characteristics of the pelagic system across Fram Strait to Kongsfjorden. Prog Oceanogr 71:182–231

Kuznetsov LL, Schoschina EV (2003) Phytocenoses of the Barents Sea (physiological and structural characteristics). Kola Scientific Centre RAS, Apatity, 308 pp (in Russian)

McMinn A, Hegseth EN (2006) Sea ice primary productivity in the northern Barents Sea, spring 2004. Polar Biol 30:289–294

McPhee MG, Proshutinsky A, Morison LH, Steele M, Alkire MB (2009) Rapid change in freshwater content of the Arctic Ocean. Geophys Res Lett 36:L10602

Nghiem SVY, Rigor IG, Perovich DK, Clement-Colon P, Weatherly JW, Neumann G (2007) Rapid reduction of Arctic perannual sea ice. Geophys Res Lett 34:L19504. doi:10.1029/2007GL031138

Pabi S, van Dijken GL, Arrigo KR (2008) Primary production in the Arctic Ocean, 1998–2006. J Geophys Res 113. doi:10.1029/2007jc004578

Ratkova TN, Wassmann P (2005) Sea-ice algae in the White Sea and Barents Sea: composition and origin. Polar Res 24:95–110

Rodrigues J (2008) The rapid decline of the sea ice in the Russian Arctic. Cold Reg Sci Technol 54:124–142

Rothrock DA, Percival DB, Wensnahan M (2008) The decline in arctic sea ice thickness: separating the spatial, and interannual variability in a quarter century of submarine data. J Geophys Res 113:C05003. doi:10.1029/2007JC004252

Sakshaug E (2004) Primary and secondary production in the Arctic Seas. In: Stein R, Macdonald RW (eds) The organic carbon cycle in the Arctic Ocean. Springer, Berlin, pp 57–81

Schauer U, Fahrbach E, Østerhus S, Rohardt G (2004) Arctic warming through the Fram Strait: oceanic heat transport from 3 years of measurements. J Geophys Res 109:C06026

Skagseth O (2008) Recirculation of Atlantic Water in the western Barents Sea. Geophys Res Lett 35:L11606

Slagstad D, McClimans TA (2005) Modeling the ecosystem dynamics of the Barents Sea including the marginal ice zone: I. Physical and chemical oceanography. J Mar Syst 58:1–18

Slagstad D, Tande KS (2007) Structure and resilience of overwintering habitats of *Calanus finmarchicus* in the Eastern Norwegian Sea. Deep Sea Res II 54:2702–2715

Slagstad D, Tande KS, Wassmann P (1999) Modelled carbon fluxes as validated by field data on the north Norwegian shelf during the productive period in 1994. Sarsia 84:303–317

Stroeve J, Holland MM, Meier W, Scambos T, Serreze M (2007) Arctic sea ice decline: faster than forecast. Geophys Res Lett 34:L09501

Tremblay JE, Gagnon J (2009) The effects of irradiance and nutrient supply on the productivity of Arctic waters: a perspective on climate change. In: Nihoul JCJ, Kostianoy AD (eds) The influence of climate change on the changing Arctic and sub-Arctic conditions. Springer, Berlin, pp 73–89

Trenberth KE, Jones PD, Ambenje P, Bojariu R, Easterling D, Klein Tank A, Parker D, Rahimzadeh F, Renwick JA, Rusticucci M, Soden B, Zhai P (2007) Observations: surface and atmospheric climate change. In: Solomon S, Qin D, Manning M, Chen Z, Marquis M, Averyt KB, Tignor M, Miller HL (eds) Climate change 2007: the physical science basis. Contribution of working group I to the fourth assessment report of the intergovernmental panel on climate change. Cambridge University Press, Cambridge

Vinje T (2001) Anomalies and trends of sea-ice extent and atmospheric circulation in the Nordic Seas during the period 1864–1998. J Climate 14:25–267

von Eye M, von Eye A, Rodrigues J (2009) Global warming and changes in Sea Ice in the Greenland Sea: 1979–2007 InterStat. Available online at http://interstat.statjournals.net/YEAR/2009/abstracts/0905003.php

Wassmann P, Bauernfeind E, Fortier M, Fukuchi M, Hargrave B, Moran B, Noji T, Nöthig E-M, Peinert R, Sasaki H, Shevchenko V (2004) Particulate organic carbon flux to the sea floor. In: Stein S, Macdonald RM (eds) The organic carbon cycle in the Arctic Ocean. Springer, Berlin, pp 101–138

Wassmann P, Slagstad D, Wexels Riser C, Reigstad M (2006a) Modelling the ecosystem dynamics of the Barents Sea including the marginal ice zone: II. Carbon flux and interannual variability. J Mar Syst 59:1–24

Wassmann P, Reigstad M, Haug T, Rudels B, Wing Gabrielsen G, Carroll ML, Hop H, Falk-Petersen S, Slagstad D, Denisenko SG, Arashkevich E, Pavlova O (2006b) Food web and carbon flux in the Barents Sea. In: Structure and function of contemporary food webs on Arctic shelves: a panarctic comparison. Prog Oceanogr 71:232–287

Wassmann P, Carroll J, Bellerby R (2008) Carbon flux and ecosystem feed back in the northern Barents Sea in an era of climate change. Deep Sea Res 55:2143–2398